

Topology Optimization, Structural & Thermal analysis and study of Harmonic Response of 3U CUBESAT in Low Earth Orbit (LEO).

A Project Report

Submitted by

Abhishek Sharma	19UMEC1102
Chitransh Soni	19UMEC1112
Ajaypal Singh Chundawat	19UMEC1103
Vikash Singh Chauhan	19UMEC1139
Krishan Kumar Sharma	19UMEC1121

Dipanshu	19UMEC1113
----------	------------

In partial fulfillment for the award of the degree

of

Bachelors of Engineering

in

Mechanical Engineering



M.B.M. UNIVERSITY

JODHPUR

June 2022

DECLARATION

This is to certify that the final year project Report titled “Topology Optimization, Structural & Thermal analysis and study of Harmonic Response of 3U CUBESAT in Low Earth Orbit (LEO) which is submitted by the students of B. E. at the Department of Mechanical Engineering at M.B.M. Engineering College, Jodhpur is a record of the candidate’s own work carried out by them under my/our supervision. The matter embodied in this report is original and has not been submitted for any other purpose. I hereby declare that this submission was their own work and that, to the best of their knowledge and belief, it contains no material previously published or written by another person nor material that to a substantial extent has been accepted for any other degree or diploma of the university or other institute of higher learning, except where due acknowledgement has been made in the text.

Declared by: -

Abhishek Sharma

Ajaypal Singh Chundawat

Chitransh Soni

Deepika Saxena

Dipanshu

Krishan Kumar Sharma

Vikash Singh Chauhan

Project guide:-

Dr. Manish Bhandari

(Assistant Professor)

Dept. of Mechanical Engineering

M.B.M. University

ACKNOWLEDGEMENT

We take immense pleasure in thanking my term project supervisor, **Dr. Manish Bhandari**, whose constant support and motivation were the driving force that kept us moving towards the goal. His suggestions helped us solve some of the critical aspects of our Project. We are deeply honoured to have him as our project supervisor. We wish to express our sincere thanks to **Dr. S.K. Singh**, professor and Head of the Department, for rendering us moral support and educating us. We are deeply indebted to them for their valuable suggestions, and advice which has resulted in the completion of the project. We would also like to thank all the Department's Teaching and Non-Teaching staff for their support. Also, we are delighted to express our gratitude to our family members and Friends whose moral support made us achieve this feat.

Abhishek Sharma

Ajaypal Singh Chundawat

Chitransh Soni

Deepika Saxena

Dipanshu

Krishan Kumar Sharma

Vikash Singh Chauhan

CONTENTS

Title	Page No.
Abstract	5
List of tables	6
List of figures	7
1. Introduction	8
2. Literature Survey	9
3. Theoretical Formulation	11
3.1 Heat Transfer Fundamentals	11
3.2 Heat balance estimation	12
4. Problem Formulation	13
4.1 Satellite Thermal Control	13
4.2 Objective	14
4.3 Thermal control design Aspects	14
4.3.1 Thermal Environment	14
4.3.2 temperature requirement of spacecraft	15
4.3.3 spacecraft Configuration	15
4.4 Thermal Control Solutions	18
5. Market Survey	21
6. Results and Discussion	22
6.1 Static Structural Analysis	22
6.1.1 loading and boundary conditions	22
6.1.2 material selection	23
6.1.3 Static Structural simulation	23
6.2 Thermal Analysis	25
6.2.1 loading and boundary conditions	26
6.2.2 material selection	26
6.2.3 Thermal simulation and theoretical validation	26
6.3 Topology Optimization	28
6.3.1 loading and boundary conditions	28
6.3.2 solution information	28
6.4 Harmonic Response Analysis	31
6.4.1 loading and boundary conditions	31
6.4.2 solution information	32
7. Conclusion	40
8. Scope for Future Work	41
9. References	41

Abstract

In this project, we design the 1U CubeSat and analyze the behaviour of a selected Aluminium 6061T6 alloy CubeSat frame subjected to static loads using finite element analysis. Failures of CubeSats due to instability caused by the G-force during launch can result in damage to the CubeSats and Launch Vehicle. Hence there is the need to analyze the maximum von-mises stress and deformation of the CubeSat before production and launch to avoid these failures and losses. The CubeSat is modelled using SolidWorks and analysis has been carried out in ANSYS 2021 R1. Finally, the results obtained are an indication of whether or not the structure is able to safely withstand the worst-case scenario static loading. We also carry out the topological optimization in order to minimize the mass. This project introduces the conceptual design and analysis of a 3U standard CubeSat in lower earth orbit. The behaviour of a selected Aluminium 6061-T6 3U CubeSat frame in the Lower Earth Orbit has been studied and the temperature and heat flux results for the worse hot case are projected using Ansys and validated with the theoretical calculations. Also, we discuss the various active and passive methods that can be incorporated in order to keep the satellite within permissible temperature limits. The topology optimization has been carried out to minimize the mass of the structure subject to deformation constraints. Further we also study the harmonic response and analyse the potential overlapping deformation patterns of excitation and natural frequencies in order to avoid resonance conditions.

List of Tables

Table No.	Title	Page No.
1	Heat transfer equation for conduction	11
2	Important Parameters	13
3	Typical spacecraft design temperatures	15
4	Physical characteristics of 3U Cubesat structure	16
5	Material properties of materials considered for structural analysis	23
6	Structural analysis results	23
7	Thermal loads in Low Earth Orbit (Heat Sources)	26
8	Material properties of Aluminum 6061 T-6	26
9	Theoretical calculations	27
10	Optimization Region	29
11	Objective	30
12	Response Constraint	30
13	Topology Optimization Solution	30
14	Harmonic response settings	33
15	Frequency Response results chart	33

List of Figures

Fig No.	Title	Page No.
Fig. 1	Various size of cubesat	8
Fig.2	Space Thermal Environment	15
Fig. 3	External dimensions (stowed), showing internal lengths associated with bus and payload	16
Fig. 4	Various parts and assembly of a 3U CubeSat a) Chassis skeleton (frame) b) Payload cover plate assembly c) Solid baseplate dual switch assembly d) Skeleton baseplate dual switch assembly	17
Fig. 5	Meshed Solid 3U CubeSat assembly	18
Fig. 6	(a-f) Steady-state structural analysis results	25
Fig. 7	Thermal analysis results	27
Fig. 8	Topology Density Variation	29
Fig. 9	Mass response convergence in subsequent iterations	31
Fig. 10	Combined objective convergence in the subsequent iteration	31
Fig.11	Directional deformation results	32
Fig. 12	Normalized natural and vibrational frequency to detect resonance condition	34
Fig. 13	Variation of amplitude and phase angle with frequency for the applied loads	34

1. Introduction

CubeSats are minuscule satellites designed for low earth orbit (LEO) with the purpose of universities worldwide to use for space research and exploration. The size and cost of spacecraft vary depending on the application; some you can hold in your hand while others like Hubble are as big as a school bus. Small spacecraft (SmallSats) focus on spacecraft with a mass of less than 180 kilograms and about the size of a large kitchen fridge [1]. Even with small spacecraft, there is a large variety of size and mass that can be differentiated as Minisatellite, 100-180 kilograms; Microsatellite, 10-100 kilograms; Nanosatellite, 1-10 kilograms; Picosatellite, 0.01-1 kilograms and FemtoSatellite, 0.001-0.01 kilograms (NASA, 2015). CubeSats are a class of nanosatellites that use a standard size and form factor. The standard CubeSat size uses a “one unit” or “1U” measuring 10x10x10 cms and is extendable to larger sizes; 1.5, 2, 3, 6, and even 12U as shown in **fig. 1**. The shape of CubeSat is essentially a cube, with outer dimensions of 10 x 10 x 10 cm, with 3.0 mm clearance above each face of the cube for mounting exterior components such as antenna, data link and power charger inlet port. The maximum allowable mass of CubeSat is 1 kg, and it is desired that the structure be no more than approximately 30% of the total CubeSat mass and should be able to withstand a minimum of 50 g’s load [2].

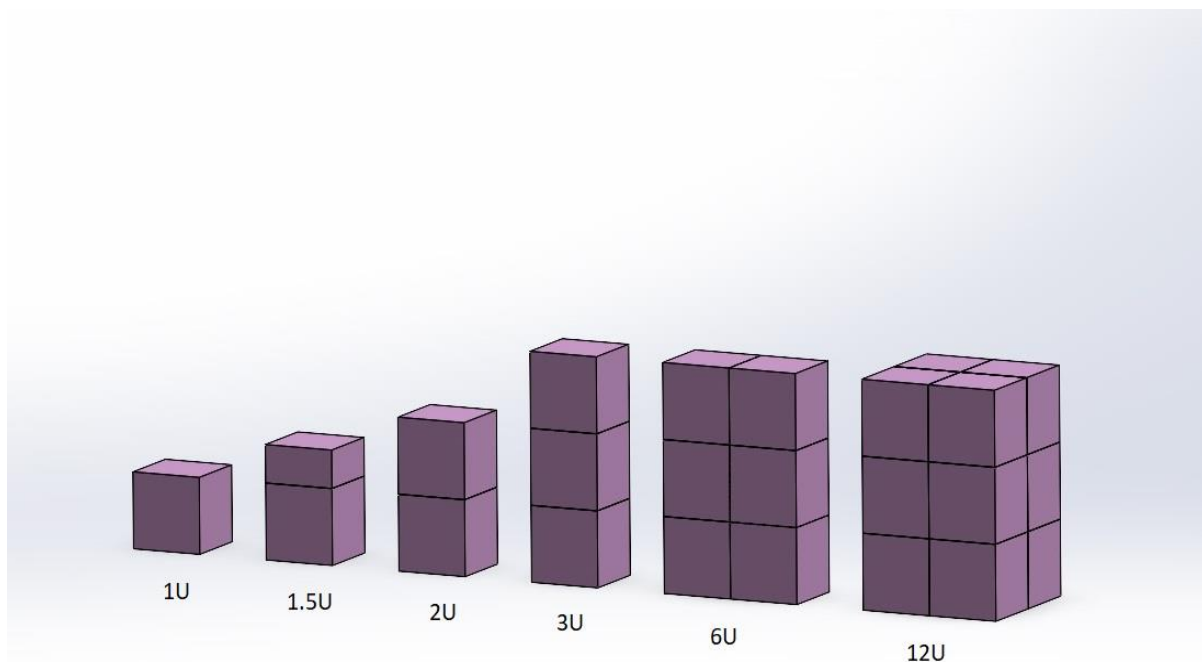


Fig. 1 Various sizes of CubeSat

Compared to traditional multi-million-dollar satellite missions, CubeSat projects have the potential to educate the participants and implement successful and useful missions in science and industry at much lower costs.

2. Literature Survey

The recent surges in advanced CubeSat missions has led to more power requirements. Therefore, resulting in new challenges of generating more power and radiating more waste heat[1]. **Young et al, [3]** discussed the most common thermal challenges like limited radiator size, adequate view factor, and limited power for heater control which occur while designing a small satellite. They demonstrated four CubeSat mission examples (TEMPEST-D, 6U; HaloSat, 6U; CubeRRT, 6U and RAVAN, 3U) and put forward guidelines to improve thermal performance. The small satellites are subjected to more severe On orbit temperature swings due to reduced thermal inertia (small mass) therefore thermal control is a deterministic factor in the final spacecraft design. The varying orbital heat loads make the satellite vulnerable to temperature fluctuations pertaining to its small mass and make thermal control a necessary and challenging task for nano satellites in low earth orbit.[9] **Blake A. Moffitt [4]** describes the thermal analysis of The Combat Sentinel Satellite (CSSAT). A thermal model is developed using the SDRC Ideas Thermal Model Generator (TMG) and expected temperatures during extreme orbital heating environments are extrapolated. Through the combined efforts of Stanford University and California Polytechnic State University, the CubeSat standard was created. A 1U unit standard CubeSat is essentially a $10 \times 10 \times 10 \text{ cm}^3$ structure with a weight up to 1.33 kg.[5] Traditionally CubeSats were envisioned merely as tools for educational purposes and demonstration. However recent trends show its transformation to real commercial missions of high value and much greater capabilities. The reduced cost and complexity and the success of smaller CubeSats (1U and 3U unit) have inspired the researchers for the development of much advanced standards for larger CubeSats (6U, 12U and 27U units CubeSat)[6]. **Reiss et al.[7]** presented a novel methodology, specific to the thermal modeling and analysis of CubeSats by utilizing a thermal software tool based on MATLAB. They demonstrated its application for the thermal analysis of UKube-1 CubeSat and compared the results with those of professional software ESATAN-TMS. The development of SLUCUBE nano-satellite developed by The Space Systems Research Laboratory (SSRL) at Saint Louis University is an attempt to provide space access to academia and commercial entities by developing low-cost,

high-risk-missions using unique commercial-off-the-shelf components which demonstrate better capability and performance [8].

The reduced development time and cost have opened the doors of space exploration to undergraduate and graduate students and commercial players. The three main operating phases of the CubeSat are launch, mission lifetime, and re-entry self-destruction.[14]. **Karthigesu Thanarasi**[17] conducted a Thermal Analysis of CUBESAT in Worse Case Hot and Cold Environment using the FEA Method by employing MSC Nastran Patran software. They suggested the use of thermal tapes and coatings over Multi-Layer Insulation (MLI) due to the fact that the side of the CubeSat frame forms an interface with the launch adapter and unlike MLI, coatings do not consume much space as well. **Athirah et al** [19] carried out the static structural analysis to study the impact of G-force during the launch process and the thermal analysis of 1U CubeSat. They draw comparisons between various designs, highlighting their advantages and disadvantages and their suitability specific to mission requirements. **S. Corpino et al**[20] carried out the thermal design and analysis of a nano satellite in low earth orbit and plot the temperature profile under dynamic conditions. Finally, the results have been discussed in-depth and found that passive thermal control methods are sufficient to keep most of the spacecraft components within their survival temperature limits provided proper thermal coatings and insulation. Nanosatellites are exposed to harsh spatial thermal conditions and to ensure its survivability and reliable operation under such conditions, **Julio Balanzá et al** [21] demonstrated the design and static structural analysis of a standard 3U CubeSat using Finite element analysis and results validated with hand calculations. In order to ensure the survivability of the nanosatellite subject to severe launch conditions and hazardous space environment they also carried out the buckling and vibrational analysis. With the increasing advancements and higher power demands, CubeSats these days employ solar cells on their surface and some are also equipped with additional deployable solar panels with fixed end angle.[9]. **Selčan et al**[22] presented advanced radiation protection technique, Fault detection, Isolation and Recovery(FDIR) for Commercial-Off-the-Shelf (COTS) based spacecraft in order to increase their reliability beyond the low earth orbit (LEO) where it is subjected to harsher environmental conditions, without compromising with the low cost and short development cycle of the nano-satellites. For thermal design, the extreme case scenario is taken into consideration i.e., the worse hot case characterized by maximum external heat loads and maximum internal dissipation and the worse cold case characterized by eclipse zones and

minimum internal dissipation. **Hengeveld et al [23]** addressed the design challenges, which prevent the widespread usage of high-power small-scale satellites for space missions. They showed that realistic deployable radiator designs have an edge over body-mounted radiator designs. Increased advancements in technology have resulted in nanosatellites with greater capabilities and power requirements. Luis A. Reyes et al[24] studied the thermal behavior of a CubeSat type nanosatellite, CIIISat and evaluated the effect of Thermal Barrier Coatings(TBC) and orbital elements(OE) on the thermal behavior of the system using a self-developed numerical code and pre-validated the results obtained with those of commercially available FDM software and further validated with experimental data from previous literature.

In this project we will study the structural, thermal and harmonic response of a selected Aluminium 6061-T6 3U CubeSat frame in the Lower Earth Orbit. The obtained results of thermal analysis will be validated with the theoretical calculation. Also, the topology optimization of the structure will be carried out in order to minimize its mass under the displacement constraint.

3. Theoretical Formulation

3.1 Heat Transfer Fundamentals

Conduction

Conduction is the process by which heat is transferred through the solid, liquid, or gas from a high energy source to a relatively lower energy source. Conduction heat transfer can occur within a material, or from two or more contacting bodies. It is governed by Fourier's Law as follows:

$$Q = -KA \frac{\delta T}{\delta x}$$

Where K: Thermal conductivity, A is the area of cross-section resisting the heat flow and $\frac{\delta T}{\delta x}$ is the temperature gradient.

Table. 1 Heat transfer equation for conduction

Formula	Coordinate
$Q = -\frac{kA(T_1 - T_2)}{\Delta x}$	Rectangular

$Q = \frac{2\pi kL(T_1 - T_2)}{\ln(D_o/D_i)}$	Cylindrical
$Q = \frac{4\pi kR_iR_o(T_1 - T_2)}{R_o - R_i}$	Spherical

Convection

$$Q = h * A * \Delta T \quad [1]$$

- h = heat transfer coefficient
- Important to spacecraft during launch after fairing separation.
- Convective heat transfer is used in some pumped-liquid thermal control systems, especially in manned spacecraft.

Radiation

Heat transfer occurs by radiating the heat between two or more surfaces through space by electromagnetic waves. It is dependent on the temperature and the coating of the radiating surface. The radiation heat transfer is governed by Stefan Boltzmann's Law as follows :-

$$Q = \sigma \varepsilon A (T_1^4 - T_2^4) \quad [2]$$

Where σ is Stefan Boltzmann's constant = $5.678 \times 10^{-8} \text{ W/m}^2\text{K}^4$ and ε is the emissivity of the surface. Radiation also occurs between solar panels and deep space. Unless the differential temperature between two or more bodies is high, radiation heat transfer is often very low. For example, the radiation energy between the sun and the spacecraft was taken into consideration for the external analysis of the CubeSat. However, the radiation between the internal electronics could be neglected because the maximum heat dissipation was only a fraction of 1 W of power.

3.2 Heat balance estimation

The Energy balance equation will be used to know the equilibrium temperature of CubeSat in two cases; hot case and cold case. With that information, we can now get the equilibrium temperatures assuming a steady-state of the hot and the cold case. The hot case is when the spacecraft is exposed to all heat sources, whereas the cold case is when the satellite passes the shadow of the earth. Then there is no influence of albedo or sunlight.

From a generalized heat balance equation for conservation of energy:

$$Q_{in} = Q_{out} \quad [3]$$

$$Q_{external} + Q_{internal} = Q_{radiated} \quad [4]$$

where,

$Q_{external}$ = Environmental heat absorbed

$Q_{internal}$ = Power dissipation by the internal electronics

$Q_{radiated}$ = Heat rejected from the spacecraft to deep space.

Direct Sunlight + Earth Emission + Albedo + Internal Heat Source = Heat radiated to deep space

$$\alpha_{sun}A_{sun}G_{sun} + \alpha_{earth}A_{earth}G_{earth} + a \times \alpha_{sun}A_{sun}G_{sun} + q_{internal} \times volume = \sigma \epsilon AT^4 \quad [5]$$

Factor	Description	Value	Unit	Remarks
α_{sun}	Solar absorptivity	0.38		Aluminum 6061-T6
A_{sun}	Area facing the sun	0.01	$[m^2]$	Top Face
G_{sun}	Solar constant	1371	$[W/m^2]$	
α_{earth}	Earth infrared absorptivity	0.38		
A_{earth}	Area facing the earth	0.01	$[m^2]$	Bottom Face
G_{earth}	Earth infrared emission	230	$[W/m^2]$	
a	Albedo	0.3		30%
$q_{internal}$	Internal heat dissipation	1	$[W/m^3]$	
σ	Stefan-Boltzmann constant	5.67×10^{-8}	$[Wm^{-2}K^{-4}]$	
ϵ	Emissivity	0.08		Aluminium 6061-T6
A	Total emitting surface area	0.14	$[m^2]$	
T	Satellite temperature		[K]	

Table. 2. Important Parameters [17]

4. Problem Formulation

4.1 Satellite Thermal Control

The role of the thermal control system is to keep the temperature of the spacecraft components within required temperature limits for given orbits, power demand, operations, and other considerations. The thermal control system should also reduce temperature gradients across the spacecraft and some components like lenses. Two temperature limits are typically defined when considering temperature control of thermal systems: an operational limit and a survival limit. An effective thermal control system will keep the component temperatures within their operational limits. A component should not lose operability within the survival limit even at extreme temperatures. The survival limit typically 10°C is wider than the operational limit. The aim of a spacecraft thermal control system (TCS) is to maintain all the components on-board the spacecraft

within the allowable temperature limits using the minimum spacecraft resources. Furthermore, it has to guarantee the optimal performance of a component in operational conditions.

In the last few years, small satellites have changed the landscape of space missions. This project introduces the conceptual design, and analysis of a 1U standard CubeSat in lower earth orbit. The behaviour of a selected Aluminium 6061-T6 1U CubeSat frame in the Lower Earth Orbit has been studied and the temperature and heat flux results for the worse hot case and the worse cold case are projected using Ansys and validated with the theoretical calculations.

The two main tasks under the responsibility of the thermal control system team are :-

1. Definition of the thermal hardware of the spacecraft and
2. Prediction of the temperatures experienced during the orbit.

4.2 Objective

The primary goals of thermal management are to:

1. Keep spacecraft components like bus/payload/battery within temperature limits. This requires the identification of factors, which affect the component temperatures and managing these factors.
2. Support the structural integrity of the spacecraft considering all external conditions, that is, external panels facing the Sun, and facing deep space.
3. Determine the effects of a short-term temperature excursion, which go beyond the design limits on component integrity and performance.
4. Provide redundancy in thermal management.

4.3 Thermal control design Aspects

The major factors driving thermal control system design are basically:

4.3.1 Thermal Environment

Spacecraft are subjected to highly variable environmental conditions. Thermal control is a process of energy management in which environmental heating plays a major role. There are three main operating phases concerning the thermal environment of the CubeSat :-

- (1) launch,

- (2) mission lifetime, and
- (3) re-entry self-destruction.

The principal forms of environmental heating on orbit are direct sunlight, sunlight reflected of Earth (albedo), and infrared (IR) energy emitted from Earth as shown in **Fig. 2**. The temperature of the satellite is the result of a balance between absorbed and emitted energy of all of these sources. There are three main sources of heat for general spacecraft systems operating in the near-Earth environment, which include the radiated heat from the sun, the albedo (the reflection of solar radiation) and planetary heating from the Earth (black-body radiation of the Earth).

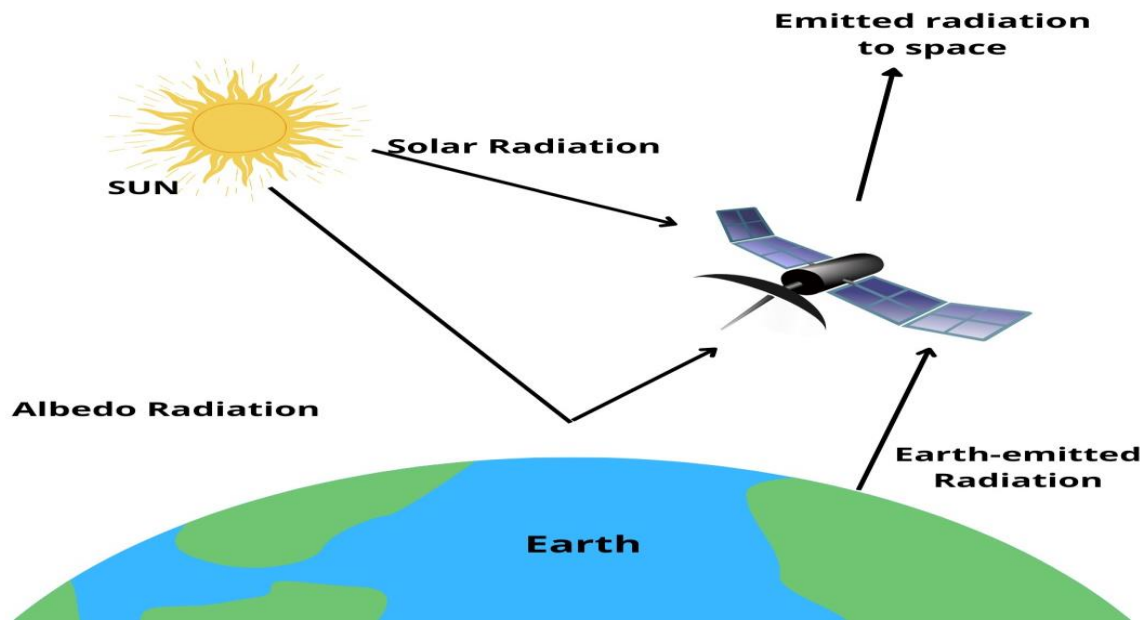


Fig.2. Space Thermal Environment

4.3.2 Temperature requirements of the spacecraft components

Table. 3. Typical spacecraft design temperatures [17]

Component/ System	Operating Temperature (C)	Survival Temperature (C)
Digital electronics	0 to 50	-20 to 70
Analog electronics	0 to 40	-20 to 70
Batteries	10 to 20	0 to 35
IR detectors	-269 to -173	-269 to 35
Solid-state particle detectors	-35 to 0	-35 to 35
Momentum wheels	0 to 50	-20 to 70
Solar panels	-100 to 125	-100 to 125

4.3.3 Spacecraft configuration.

The geometric configuration of the standard 3U CubeSat structure is shown in **fig.3-4** For the discretization, the meshing parameters used are tetrahedron-type elements having 70 mm average dimension. It results a number of 20110 nodes and 10978 elements(**fig.5**).

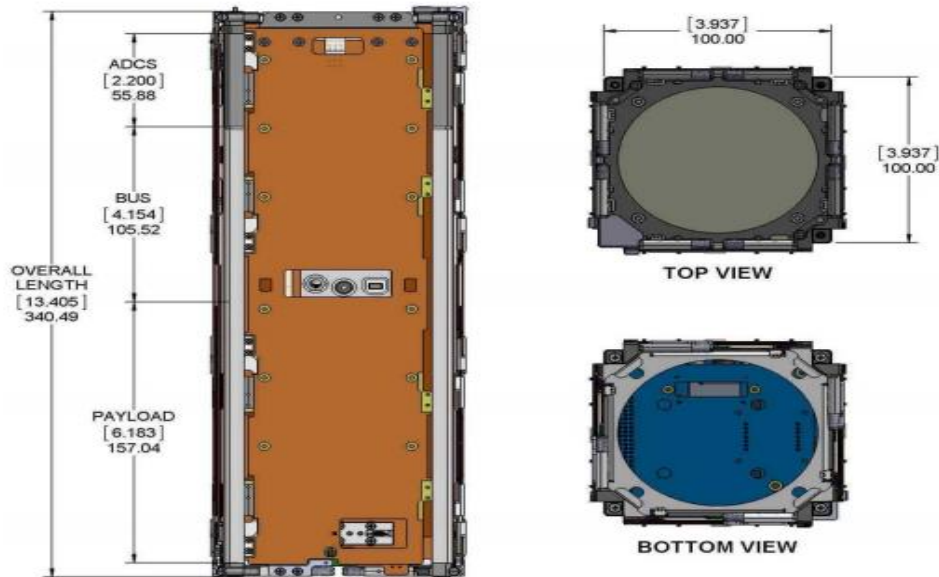
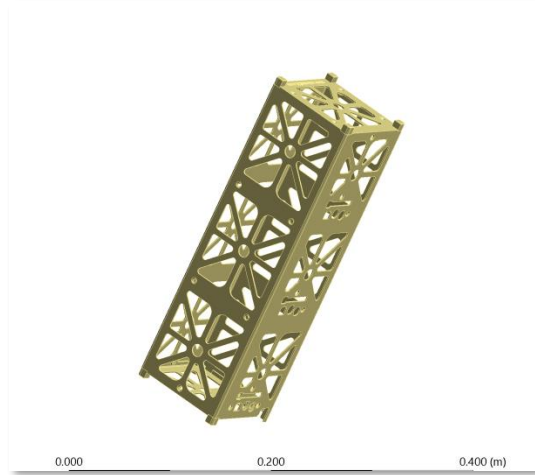


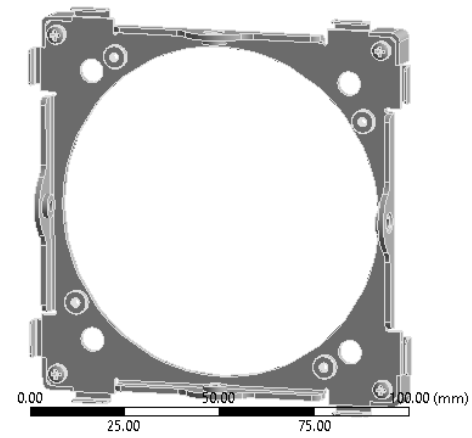
Fig.3 External dimensions (stowed), showing internal lengths associated with bus and payload [12]

Table 4. Physical characteristics of 3U Cubesat structure [12]

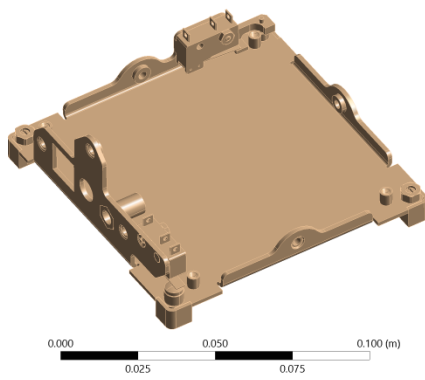
Parameter	Conditions / Notes	Symbol	Min	Typ	Max	Units
Mass	Estimated, when outfitted in "propeller" configuration with four fixed and eight deployable solar panels.			2800		g
Overall length (Z)	Conforms to CubeSat specification			340.5		mm
Overall width (X)				100.0		
Overall depth (Y)				100.0		
Aperture on zenith end				88		mm



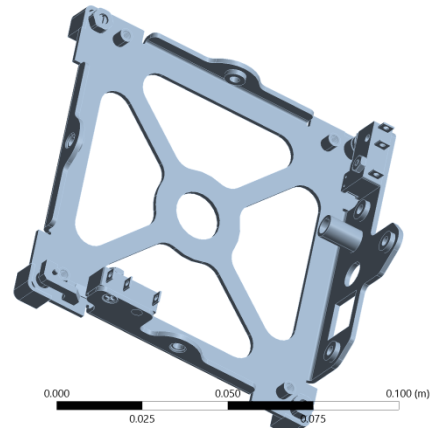
a



b



c



d

Fig.4 Various parts and assembly of a 3U CubeSat. a) Chassis skeleton (frame) b) Payload cover plate assembly c) Solid baseplate dual switch assembly d) Skeleton baseplate dual switch assembly

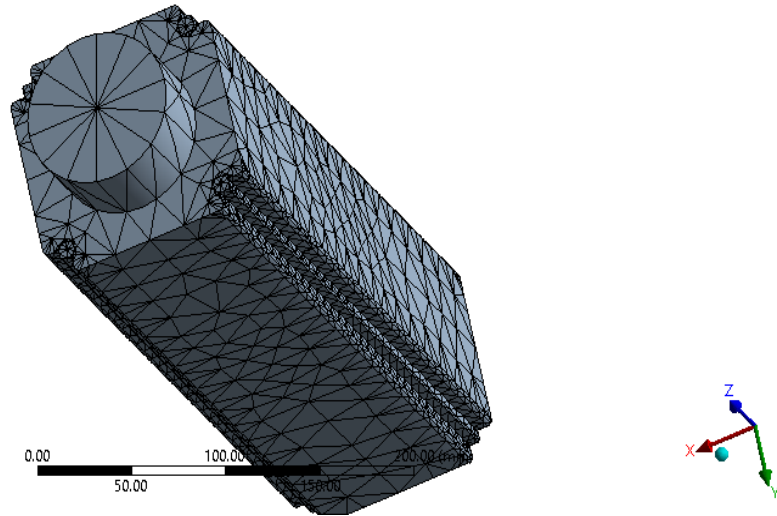


Fig. 5 Meshed Solid 3U CubeSat assembly

4.4 Thermal Control solutions

The thermal control can be passive or active depending on the design approach. Passive control is applied to most of the nano-satellites because of the simplicity, cost, reliability, limited mass, and power. In order to maintain the temperature of the components within the allowable temperature range, and minimize the mass and power requirements, the thermal design is a key step to be taken at the beginning of the program.

4.4.1 Passive Systems

Passive thermal control requires no input power for the thermal regulation of a spacecraft. This can be achieved using several methods and is highly advantageous to spacecraft designers, especially for the CubeSat form factor, as passive thermal control systems are associated with low cost, volume, weight, and risk, and due to their simplicity have been shown to be highly reliable. The integration of Multi-Layer Insulation (MLI), thermal coatings/surface finishes, heat pipes, sunshades, thermal straps and louvers are some examples of passive methods to achieve thermal control in a spacecraft.

➤ *Films, Coatings, and Thermal Insulation*

In a vacuum, heat is transferred by two means: radiation and conduction. The internal environment of a fully enclosed small satellite is usually dominated by conductive heat transfer, while heat transfer to/from the outside environment is driven via thermal radiation. Thermal radiation heat transfer is controlled by using materials that have certain specific radiative properties, namely: solar absorptivity (implying wavelengths in the range of $\sim 0.3 - 3 \mu\text{m}$) and, IR (infrared) emissivity ($\sim 3 - 50 \mu\text{m}$) Thermal insulation is used as a thermal radiation barrier from incoming solar or IR flux and/or to prevent undesirable radiative heat dissipation. Commonly used to maintain temperature ranges for electronics and batteries in-orbit, or more recently, for biological

payloads, thermal insulation is usually in the form of MLI blankets. However, the use of metallized tapes is also common for small spacecraft applications.

➤ **Multi-layer insulation, or MLI**

It is thermal insulation composed of multiple layers of thin sheets that are often used on spacecraft. It is one of the main items of the spacecraft thermal design, primarily intended to reduce heat loss by thermal radiation. The principle behind MLI is that of radiation shields; to reduce the overall heat transfer coefficient between two radiating surfaces materialsthat are highly reflective. It is introduced between the heat-exchanging surfaces. The radiation shield reduces the radiation heat transfer by effectively increasing the surface resistances without actually removing any heat from the overall system. [5] When two bodies at different temperatures are kept at a certain distance of d from each other, there are three resistances that come into play.

- Surface resistance of body 1 given in Equation $r_{surface} = \frac{1-\epsilon}{A\epsilon}$

Where, ϵ is the emissivity of the object and A is area of radiating surface.

- Space resistance due to the space in between the two bodies. $r_{space} = \frac{1}{A_1 F_{1-2}}$

When a radiation shield is introduced in between two surfaces it causes an increase in resistance by increasing the surface resistance due to introduction of two extra surfaces as well as a conductive resistance.

➤ **Sunshields**

The use of a sunshield, or sunshade, is common for spacecraft thermal control, although only recently has this been implemented on small spacecraft to improve thermal performance.

➤ **Thermal Straps – Passive**

Recently, flexible thermal straps have become a convenient way to control temperature on small spacecraft, as the required mass for the strap is reduced and there is reduced stiffness between components. Flexible thermal straps can be used to allow for passive heat transfer to a thermal sink and can be customized to any particular length required.

➤ **Thermal Louvers**

Although commonly defined as active thermal control, here we consider louvers as a passive thermal control component because the designs considered do not require a power input from the spacecraft. Full-sized louvers for larger spacecraft have high efficacy for thermal control; however, their integration with small spacecraft has been challenging. Typical spacecraft louvers are associated with a larger mass and input power, which are both limited on small spacecraft.

➤ **Deployable Radiators**

A passive deployable radiator that is lightweight and simple in design would greatly enhance thermal performance by increasing the available radiative surface area. Similar to thermal louvers, using deployable radiators on small spacecraft is challenging due to volumetric constraints.

➤ *Deployable Solar Arrays*

Deployable solar arrays may also provide a thermal design advantage as solar cells mounted away from the body of small satellite allow for optimized surface coatings to provide improved thermal control as well as improved cooling of the array. A typical solar cell α/ϵ ratio may approach unity making heat rejection difficult in hot attitudes with direct or reflected solar flux incident upon the spacecraft. Also, deployed solar arrays would be able to radiate off a high emissivity/low solar absorptance backside for improved thermal management of the array.

➤ *Heat Pipes*

Heat pipes are an efficient passive thermal transfer technology, where a closed-loop system transports excess heat via temperature gradients, typically from electrical devices to a colder surface, which is often either a radiator itself, or a heat sink that is thermally coupled to a radiator.

➤ *Thermal Storage Units/Phase-Change Devices*

Thermal storage units can be used in various applications for passively storing thermal energy for component protection or for future energy use. Thermal Management Technologies has developed a phase-changing thermal storage unit (TSU) that considers desired phase-change temperatures, interfaces, temperature stability, stored energy, and heat removal methodologies. A complete fabrication of this device will allow the user to control temperature peaks, stable temperatures and/or energy storage

➤ *Heat Switches*

Heat (or thermal) switches are devices that can switch between being good thermal conductors or good thermal insulators as needed to control the temperature of heat producing components.

4.4.2 Active Systems

Active thermal control methods rely on input power for operation and have been shown to be more effective in maintaining tighter temperature control for components with stricter temperature requirements or higher heat loads. Typical active thermal devices used on large-scale spacecraft include electrical resistance heaters, cryocoolers, and the use of thermoelectric coolers.

➤ *Heaters*

On small spacecraft, electrical resistance heaters are typically used to maintain battery temperature during cold cycles of the orbit and are controlled by a thermostat or temperature sensor. Biological nanosats (GeneSat, PharmaSat, O/OREOS, SporeSat, EcAMSat, and BioSentinel) all use actively-controlled resistance heaters for precise temperature maintenance for their biological payloads, with closed-loop temperature feedback to maintain temperatures.

➤ *Cryocoolers*

Cryocoolers are refrigeration devices designed to cool around 100K and below. Cryocoolers are used on instruments or subsystems requiring cryogenic cooling, such as high precision IR sensors. Further, the use of cryocoolers is associated with longer instrument lifetimes, low vibration, high thermodynamic efficiency, low mass, and supply cooling temperatures less than 50K.

5 Market Survey

Project Cost Estimate

Ideally in order to develop this cost estimating model we adopt, as a baseline, a 10 x 10 x 10 cm CubeSat that carries a camera and a transmission system. The satellite mass is limited to 1 kg and it requires some attitude control. The project will pass through various phases each of which should be costed separately.

Phase 1 — Project definition and initiation

This is the phase where the feasibility is studied and a working group is put together. This phase should not incur any financial expenses unless a Workshop is attended. Assuming this is done the cost will involve travel to the workshop and accommodation costs. This is estimated at US\$5,000. Documentation and specifications of CubeSats that are required.

Phase 2 — Spacecraft construction

In this phase, equipment will have to be purchased. The components to be purchased include -

Satellite frame: The ISIS CubeSat structure is developed as a generic satellite structure based upon the CubeSat standard. The design created by ISIS allows for multiple configurations to give the nanosatellite developers the freedom to develop their satellite with respect to the basic lay-out of their internal configuration — cost: 19k.

Attitude control system: A Passive Magnetic Attitude Stabilization System is selected to lock the CubeSat to the Earth Magnetic field like a compass needle — cost: 16k.

Camera system: A Sanyo VCC-5884E 1/3 in. Color CCD DSP High-Resolution Camera, 540TVL, 1 Lux Sensitivity, 12VDC/24VAC, Automatic Gain Control (ON/OFF), used for security cameras with a mass of 167 grams and size of 68 x 63 x 52 mm — cost: 7k.

Transmission system: CubeSat UHF downlink, VHF uplink full-duplex transceiver, provides telemetry, telecommand & beacon capability in a single board — Cost: 8k.

Antenna system: The ISIS deployable antenna system contains up to four tape spring antennas of up to 55 cm length, which deploy from the system after orbit insertion .

Solar cells: The Nano Power P-series power supplies are designed for small, low-cost satellites with power demands from 1-30W —5k

Phase 3 — Launch preparation

In this phase the satellite has to be transported to the launch site and placed in the special CubeSat deployer.

The transport of the satellite, along with a team member overseeing installation, is estimated at US\$5,000. Obviously, this cost is dependent on the location of the university and other factors of availability.

Phase 4 — Launch cost

It has been suggested that the launch vehicle cost is the highest cost of a CubeSat project. As

outlined above, commercial prices range from US\$40,000 to US\$2 million. In considering these prices, we should, however, remember that they are “commercial”, they typically apply to commercial satellites that are placed in orbit to generate a profit to their owners; and “prices”, which in a commercial environment are only related to the ‘cost’ to the extent that it would be nice to recover all the cost, but with the price ultimately being determined by whatever the customer is prepared to pay.

In the case of educational (i.e., non-commercial) CubeSats, it will be necessary to investigate launch cost in more detail. To get an idea of how this cost is determined Wertz⁷ has proposed the formula located at the bottom of the previous page.

Post Launch Operations

Finally, there is the cost of the operation of the CubeSat once it is launched and is in orbit. Bearing in mind that the prime objective of educational CubeSats is its function as a learning tool, and that such an objective is achieved before the launch takes place, in-orbit operation is a mere bonus, further a department that can make use of scientific data collected.

Conclusion of estimation

This, then, brings the total cost of placing an educational CubeSat in orbit at: **US\$52,000**
However, the actual cost of our basic structure- For the fabrication of the present basic structure presented in this project, (Al6061t6 sheets-rs800), (fabrication and solar panel costs18000).

6. Results and Discussion

6.1 Static structural analysis

During the process, there are mainly three types of mechanical loading acting on the CubeSat, which are: quasistatic, static and dynamic loading. The analysis of the static loading acting on the CubeSat will emphasize on the stress distribution and deformation of the CubeSat chassis.

6.1.1 Loading conditions and boundary conditions

30g load acting in the vertical direction is divided by four giving a value of 73.575 N. This means that each of the extruded pins will be loaded by a force of 73.575 N. the lowermost extruded pins represent the fixed support which will be in contact with the lower boundary of launch pad. 10g load acting in horizontal direction is divided by two, giving a value of 49.05 N. the two sides will have fixed support which will be in contact with the lower boundary of the P-Pod[19].

The structure has been subjected to a cantilever beam type boundary condition with one end fixed and one end free. It is given by

$$\text{at } x = 0, \quad u = 0 \quad v = 0; w = 0;$$

$$\theta_x = 0; \theta_y = 0; \theta_z = 0$$

Where u , v and w represent the displacement in x , y and z direction respectively and θ_x , θ_y and θ_z represent the rotation about x , y and z axis respectively.

6.1.2 Material Selection

Specifically, allowed materials are four aluminum alloys: 7075, 6061, 5005, and 5052. Furthermore, further consideration is put into material selection as not all materials can be used in vacuums. In our case, Aluminum 6061 T-6 has been taken into account for the external design of CubeSat. It has good mechanical properties, exhibits good weldability, and remains resistant to corrosion. We carry out the structural analysis for structural steel, AL-6061-T6, and AL-7075-T6.

Table 5 material properties of materials considered for structural analysis [17]

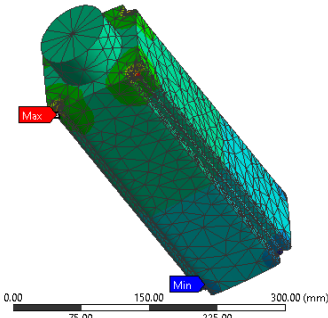
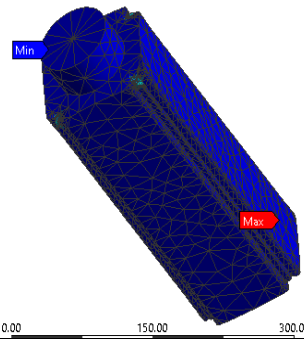
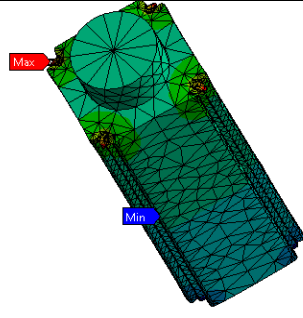
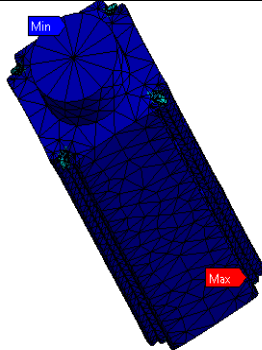
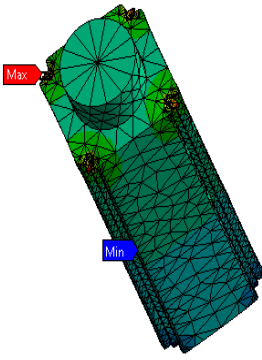
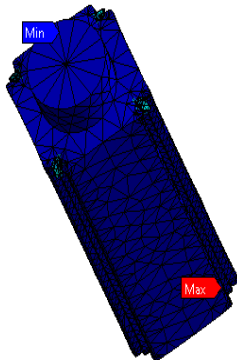
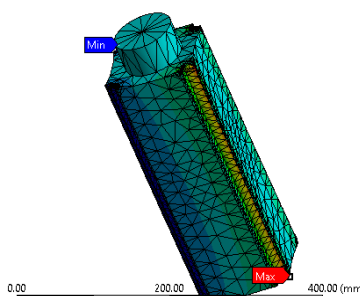
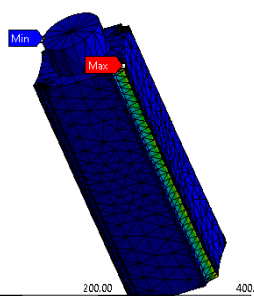
Material	Yield Strength	Density	Machinability
Structural Steel	250MPa	785kg/m ³	Easy
AL-6061-T6	320MPa	2850 kg/m ³	Easy
AL-7075-T6	340MPa	2796 kg/m ³	Easy

6.1.3 Static Structural Simulation

The obtained Max Von-mises Stress and Max Deformation for horizontal loads for Structural Steel, AL-6061-T6, and AL-7075-T6 have been summarized in **Table. 6** and **Fig 6** represents the analytical results of the same. The results provided us with max von Mises stress varying from 3.67 MPa to approximately 3.81 MPa in vertical loading conditions and around 0.137 MPa in horizontal loading conditions. The yield strength of the materials used is far above the max range of stresses induced. However further consideration is put into material selection as not all materials can be used in vacuums.

Table 6. Structural analysis results

Material	Max Von-mises Stress (MPa)	Max Deformation (e-4 mm)
Vertical load		
Structural steel	3.81	1.65
AL-6061-T6	3.67	4.81
AL-7075-T6	3.68	4.63
Horizontal load		
Structural steel	0.138	0.05
AL-6061-T6	0.137	0.156
AL-7075-T6	0.137	0.151

Vertical Load		
Material	Total Deformation	Von mises Stress
Structural Steel	<p>A: Static Structural Total Deformation Type: Total Deformation Unit: mm Time: 1 04-03-2022 11:51</p> <p>0.00016553 Max 0.00014714 0.00012874 0.00011035 9.196e-5 7.3568e-5 5.5176e-5 3.6784e-5 1.8392e-5 0 Min</p> 	<p>A: Static Structural Equivalent Stress Type: Equivalent (von-Mises) Stress Unit: MPa Time: 1 04-03-2022 11:54</p> <p>3.8118 Max 3.3883 2.9648 2.5414 2.1179 1.6944 1.2709 0.84745 0.42398 0.00050072 Min</p> 
Al7075t6	<p>A: Static Structural Total Deformation Type: Total Deformation Unit: mm Time: 1 04-03-2022 13:01</p> <p>0.00046319 Max 0.00041173 0.00036026 0.00030879 0.00025733 0.00020586 0.0001544 0.00010293 5.1466e-5 0 Min</p> 	<p>A: Static Structural Equivalent Stress Type: Equivalent (von-Mises) Stress Unit: MPa Time: 1 04-03-2022 13:03</p> <p>3.679 Max 3.2703 2.8615 2.4528 2.0441 1.6354 1.2267 0.81794 0.40922 0.00050495 Min</p> 
Al6061t6	<p>A: Static Structural Total Deformation Type: Total Deformation Unit: mm Time: 1 04-03-2022 13:06</p> <p>0.00048132 Max 0.00042794 0.00037436 0.00032088 0.0002674 0.00021392 0.00016044 0.00010696 5.348e-5 0 Min</p> 	<p>A: Static Structural Equivalent Stress Type: Equivalent (von-Mises) Stress Unit: MPa Time: 1 04-03-2022 13:09</p> <p>3.679 Max 3.2703 2.8615 2.4528 2.0441 1.6354 1.2267 0.81794 0.40922 0.00050495 Min</p> 
Horizontal Load		
Material	Total Deformation	Von mises Stress
Structural Steel	<p>A: Static Structural Total Deformation Type: Total Deformation Unit: mm Time: 1 04-03-2022 13:23</p> <p>5.4212e-6 Max 4.8188e-6 4.2165e-6 3.6141e-6 3.0118e-6 2.4094e-6 1.8071e-6 1.2047e-6 6.0235e-7 0 Min</p> 	<p>A: Static Structural Equivalent Stress Type: Equivalent (von-Mises) Stress Unit: MPa Time: 1 04-03-2022 13:26</p> <p>0.13834 Max 0.12297 0.10761 0.092238 0.07687 0.061501 0.046133 0.030765 0.015397 2.8421e-5 Min</p> 

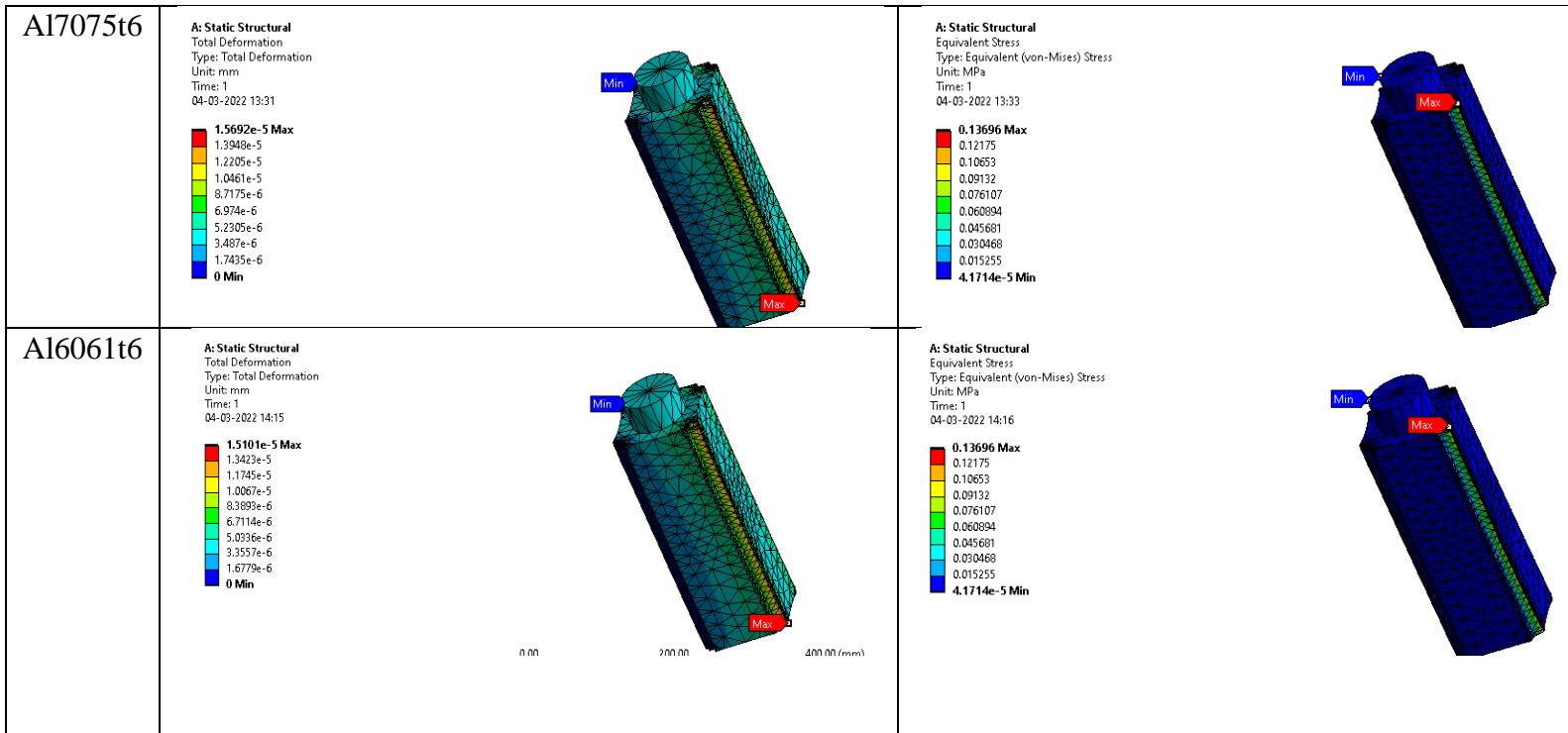


Figure 6 Static structural analysis results

In our case, Aluminum 6061 T-6 has been taken into account for the external design of CubeSat. It has good mechanical properties, exhibits good weldability and remains resistant to corrosion. The areas affected the most by the von Mises stress occur on the center of the bottom Face of the CubeSat. The test showed that the material used on the CubeSat, should be able to withstand the loads throughout the launch period. Also, when the values of the physical deformation are looked at, they only vary slightly. These values are extremely small and can be considered negligible with respect to the integrity of the structure during launch, as this set of results represents a worst-case scenario. The critical points of deformation seem to occur at the side top edges of the structure, but seem to pose no threat as the material is strong enough to withstand the loads.

6.2 Thermal Analysis

In order to size the thermal control system, the worst-case scenarios (those leading to extreme thermal loads) have to be identified. The so-called hot cases and cold cases, for operating, start-up, and survival conditions of equipment are defined this way. These dimensioning cases are defined by an appropriate combination of external fluxes (solar, albedo and planetary infrared), material properties, and unit dissipation profiles. Normally, the hot case corresponds to the maximum external loads and maximum internal dissipation. The maximum external loads usually

take place at the sub-solar point in a planetary orbit, or during the perihelion in a solar orbit. The cold case usually corresponds to eclipse zones for planetary orbits and to the aphelion phase for a solar orbit. Modes of operation with minimum dissipation are chosen to assess the cold cases. Since the dimensioning loads are defined for the worst-case scenarios, steady-state calculations under these conditions are carried out. The study of steady-state hot cases usually allows radiator sizes to be determined, while the study of SteadyState cold cases is used to assess the need of heaters, their location and power.

6.2.1 Loading and Boundary Conditions

The boundary conditions corresponding to Lower Earth Orbit are as follows: -

The temperature surrounding the satellite in space = 2.7 K[17]

Pressure surrounding is very close to vacuum Summary of the various external heat sources

Table 7–Thermal loads in Low Earth Orbit (Heat Sources) [17]

Heat source	Magnitude
Direct solar flux	1371 W/m ² (1316 - 1428)
Albedo	30% of direct solar flux
Earth infrared radiation	230 W/m ²
Energy dissipation inside spacecraft	1 W/m ³

6.2.2 Material Selection

Aluminum 6061 T-6 has been taken into account for the external design of CubeSat as not all materials can be used in vacuums.

Table 8. Material properties of Aluminum 6061 T-6[17]

Material	Absorptivity	Emissivity	Sp Heat	Density	Young's Modulus	Poisson's Ratio
Aluminium 6061 T6	0.379	0.08	875	2850	69 GPa	0.33

6.2.3 Thermal simulation and theoretical validation

➤ Worst Hot Case

The top face of the CubeSat faces the sun and receives the solar flux of 1371 W/m², the bottom face of the cubesat faces the earth and receives the earth infrared emission of 230 W/m² and albedo (30%). All six faces of the CubeSat radiate heat energy to the ambient space at 2.7 Kelvin.

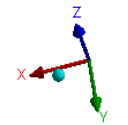
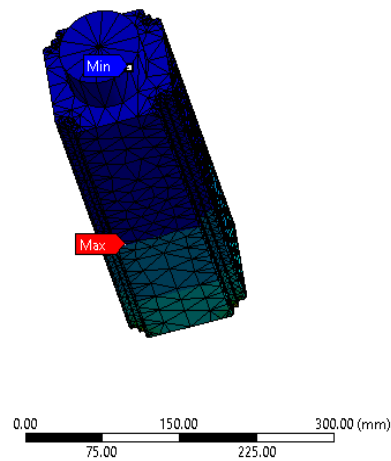
Table 9-Theoretical calculation

Formula	Value	Unit	Description
$\alpha_{sun}A_{sun}G_{sun}$	5.2098	[W]	Top plate facing sun
$\alpha_{earth}A_{earth}G_{earth}$	0.874	[W]	Bottom plate facing earth
$a \times \alpha_{sun}A_{sun}G_{sun}$	1.5629	[W]	bottom plate receiving albedo
$q_{internal}$	1	[W/m3]	Internal heat generation
$\sigma \varepsilon A$	6.3504e-10		
$T_{equilibrium}$	1092.9	[K]	
	819.9	[°C]	

A: Steady-State Thermal

Temperature
Type: Temperature
Unit: °C
Time: 1
05-03-2022 12:47

576.87 Max
534.33
491.79
449.25
406.71
364.17
321.63
279.09
236.55
194.01 Min



A: Steady-State Thermal

Total Heat Flux
Type: Total Heat Flux
Unit: W/mm²
Time: 1
05-03-2022 12:58

4.1493 Max
3.6883
3.2272
2.7662
2.3052
1.8441
1.3831
0.92209
0.46106
3.2628e-5 Min

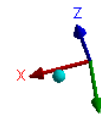
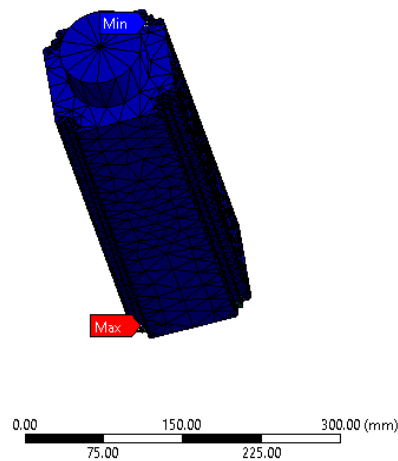


Fig. 7 Thermal analysis results

Fig.7 shows the thermal analysis results for the worse hot case, showing the total heat flux and the maximum and minimum temperatures. As we analyze the temperature fringe in the diagram above, it can be concluded that the maximum temperature obtained is 849.87 K which is equivalent to 576.87°C. That is the worst-case temperature which the CubeSat would be experiencing during the hot environment. According to the theoretical value which was calculated earlier as shown in Table 9, it's proven via calculation that the worst-case hot scenario is 819.9 °C or 1092.9K. The maximum heat flux experienced by the CubeSat during worst hot case is found to be 4.139 W/mm². So the simulated temperature range is within the calculated theoretical temperature value which is 1092.9 K. Also, the attained temperature during worse hot case is lower than the melting temperature of AL-6061-T6 (585 °C). Thus, the worse hot case working temperature is within the calculated temperature. It shows that the CubeSat would not fail and will remain fully operational throughout its lifespan.

6.3 Topology Optimization

Topology optimization is a mathematical method that optimizes material layout within a given design space, for a given set of loads, boundary conditions, and constraints with the goal of maximizing the performance of the system. Topology optimization is different from shape optimization and sizing optimization in the sense that the design can attain any shape within the design space, instead of dealing with predefined configurations.

The conventional topology optimization formulation uses a finite element method (FEM) to evaluate the design performance.

6.3.1 Loading and boundary conditions

Topology Optimization is most commonly used for objective such as maximization of stiffness, separation of eigenfrequencies and minimization of mass. Here our objective is to minimize the mass. A static load of 1000 N has been applied at the free end, considering cantilever structure. Boundary conditions as given by

$$atx = 0, \quad u = 0; v = 0; w = 0;$$

$$\theta_x = 0; \theta_y = 0; \quad \theta_z = 0$$

Where u, v and w represent the displacement in x, y and z direction respectively and θ_x, θ_y and θ_z represent the rotation about x, y and z axis respectively.

6.3.2 Solution information

Here we have optimized the mass of our structure by keeping displacement as a constraint and have successfully achieved a resolved structure with 24 percent reduced mass, hence retaining 76

% of the structural mass. **Fig 8** shows the topology optimized structure, also the results of mass convergence in subsequent iterations have been plotted in **Fig 9**. It suggests that we have achieved a significant convergence in the very first iteration itself. Subsequent iterations cause no further reduction in mass. As the stresses generated are minimum at the free end of the cantilever, therefore the end near the p-pod is suited for maximum material removal.

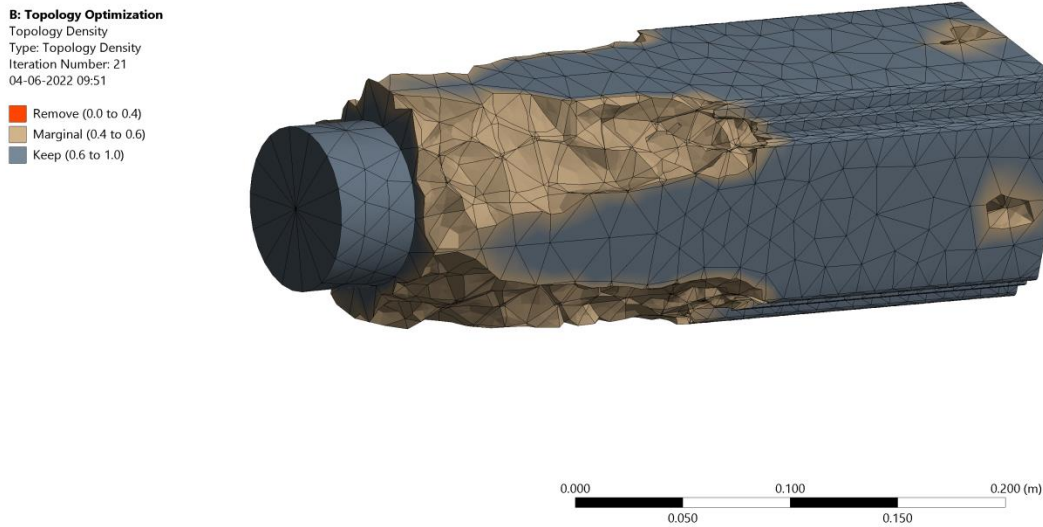


Figure 8 Topology optimized structure

TABLE 10 Optimization Region

Object Name	<i>Optimization Region</i>
State	Fully Defined
Design Region	
Scoping Method	Geometry Selection
Geometry	All Bodies
Exclusion Region	
Define By	Boundary Condition
Boundary Condition	All Boundary Conditions
Optimization Option	
Optimization Type	Topology Optimization - Density Based

TABLE 11 Objective

Response Type	Goal	Formulation	Environment Name	Weight	Multiple Sets	Start Step	End Step	Step	Start Mode	End Mode	Mode
Compliance	Minimize	Program Controlled	Static Structural	N/A	Enabled	1	1	1	N/A	N/A	N/A

TABLE 12 Response Constraint

Object Name	<i>Response Constraint</i>
State	Fully Defined
Scope	
Scoping Method	Optimization Region
Optimization Region Selection	Optimization Region

TABLE 13 Topology Optimization Solution

Object Name	<i>Solution Information</i>
State	Obsolete
Solution Information	
Solution Output	Objective & Mass Response Convergence
Update Interval	2.5 s
Display Points	All
Definition	
Type	Response Constraint
Response	Mass
Define By	Constant
Percent to Retain	76 %
Suppressed	No

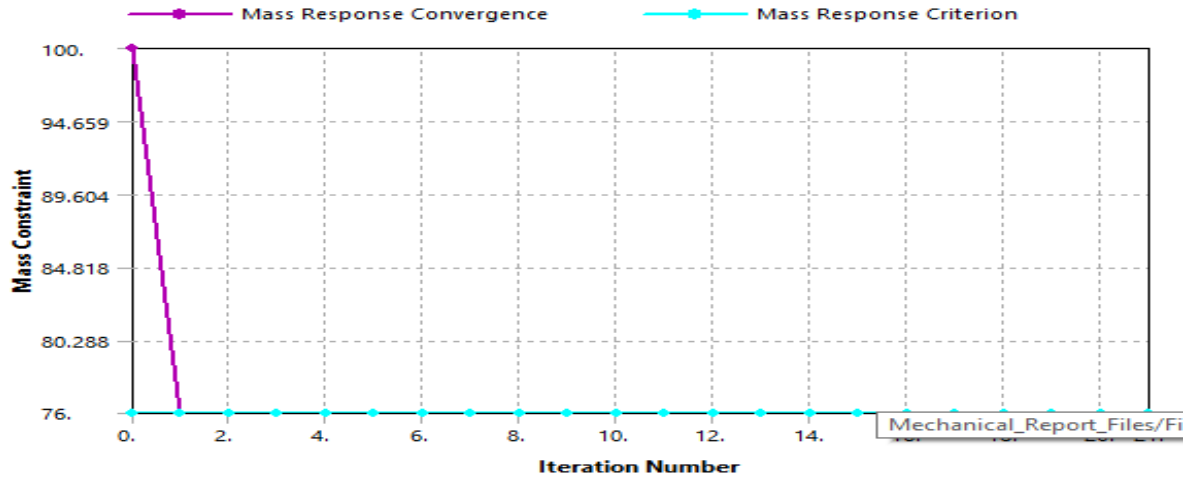


Fig 9. Mass response convergence in subsequent iterations

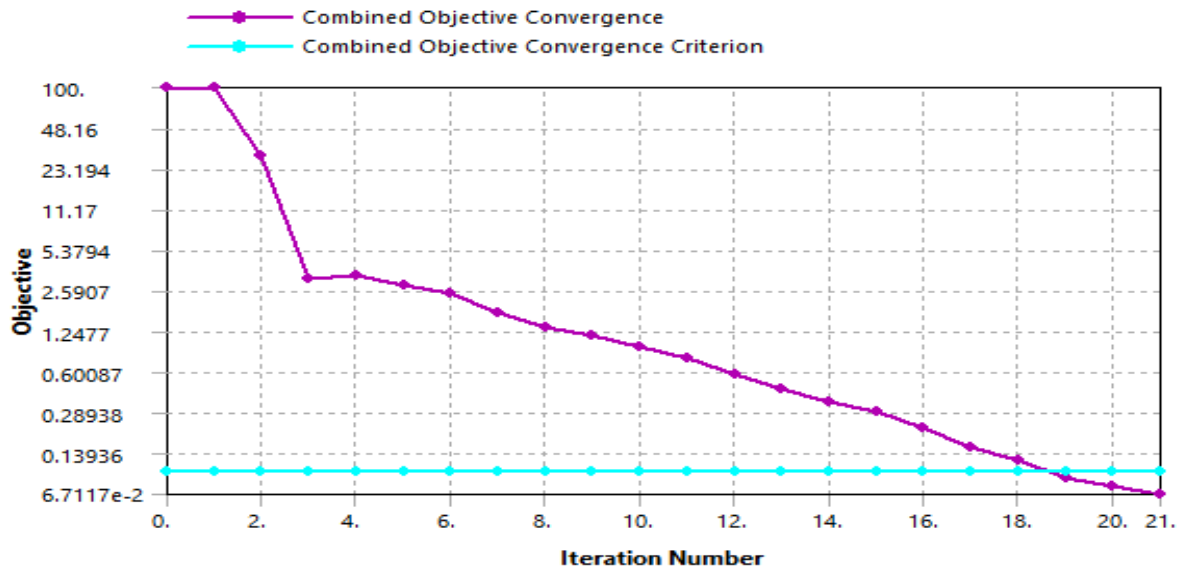


Figure 10 Combined objective convergence in subsequent iteration

The Combined objective convergence shows a steep decline in a range of 100 to 2.5 in the first three iterations (**Fig.10**). Whereas subsequent iterations cover a not so considerable range. This was expected as we get almost all the mass optimization in the initial iterations themselves, therefore further iterations do not possess considerable importance. Further fatigue life, damage, safety factor, maximum stress, deformation, and also weight of the standard 3U CubeSat model can be investigated for all alternative models designed in subsequent iterations.

6.4 Harmonic response Analysis

In this project, the harmonic response of a standard 3U CubeSat is investigated by using the finite element analysis method in Ansys workbench.

6.4.1 loading and boundary conditions.

Using the same loading and boundary conditions as in structural analysis, the vibrational stability of the structure is investigated for a frequency range of 0 to 1000 HZ using the full method.

B: Harmonic Response

Directional Deformation

Type: Directional Deformation(Z Axis)

Frequency: 1000. Hz

Sweeping Phase: -164.84 °

Unit: mm

Global Coordinate System

14-05-2022 11:31

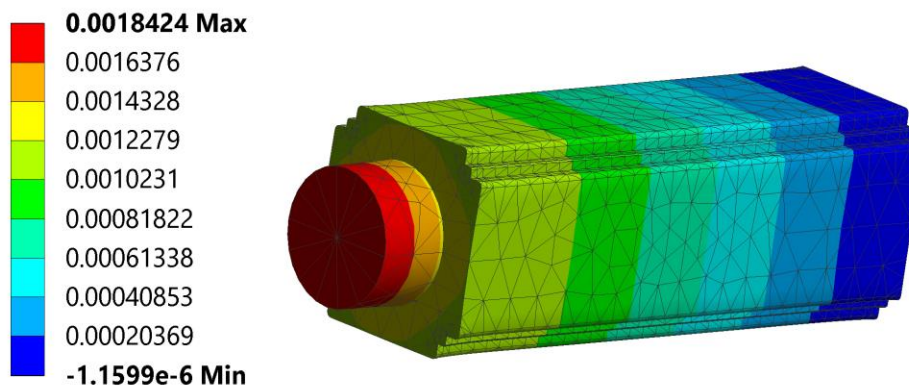


Figure 11 Directional deformation results

6.4.2 Solution information

Our objective for carrying out the harmonic response analysis is to investigate the occurrence of resonance phenomenon of the standard 3U CubeSat structure by comparing natural frequency and the vibration frequency during the launch phase, with the purpose to avoid resonance which could negatively influence to strength and stability of the structure. Here we have used the full method for harmonic response analysis and obtain the directional deformation results (**fig. 11**), however an alternate method could be to first, conduct modal analysis and obtain the natural vibration frequencies and the response effect under each natural vibration frequency.

Table 14 Harmonic response settings

Object Name	<i>Directional Deformation</i>
State	Solved
Scope	
Scoping Method	Geometry Selection
Geometry	All Bodies
Definition	
Type	Directional Deformation
Orientation	Z Axis
By	Frequency
Frequency	1000. Hz
Amplitude	No
Sweeping Phase	-164.84 °
Coordinate System	Global Coordinate System

Table 15 Frequency Response results chart

Object Name	<i>Frequency Response</i>
State	Solved
Scope	
Scoping Method	Geometry Selection
Geometry	1 Vertex
Spatial Resolution	Use Average
Definition	
Type	Directional Deformation
Orientation	Z Axis
Coordinate System	Global Coordinate System
Suppressed	No
Options	
Frequency Range	Use Parent
Minimum Frequency	0. Hz
Maximum Frequency	1000. Hz
Display	Bode
Chart Viewing Style	Log Y
Results	
Maximum Amplitude	1.1552e-003 mm
Frequency	1000. Hz
Phase Angle	164.84 °
Real	-1.115e-003 mm
Imaginary	3.0215e-004 mm

Fig12 shows a combined graph of normalized natural and vibrational frequencies for a considered frequency domain of 0 to 1000 Hz. There occur a resonance condition at 728 Hz. This could be avoided by taking various measures like adding stiffness to the structure which would lead to an increase in the natural frequency. Also we could retain more mass during topology optimization which would decrease the natural frequency. If none of this be possible, we can reduce the forcing amplitudes, which in turn would reduce the response at resonance. We also see a parabolic decline in phase angle with increase in frequency and a parabolic increase in amplitude with increase in

frequency (**fig. 13**). This significant surge in amplitude is indicative of the occurrence of resonance at higher frequencies.

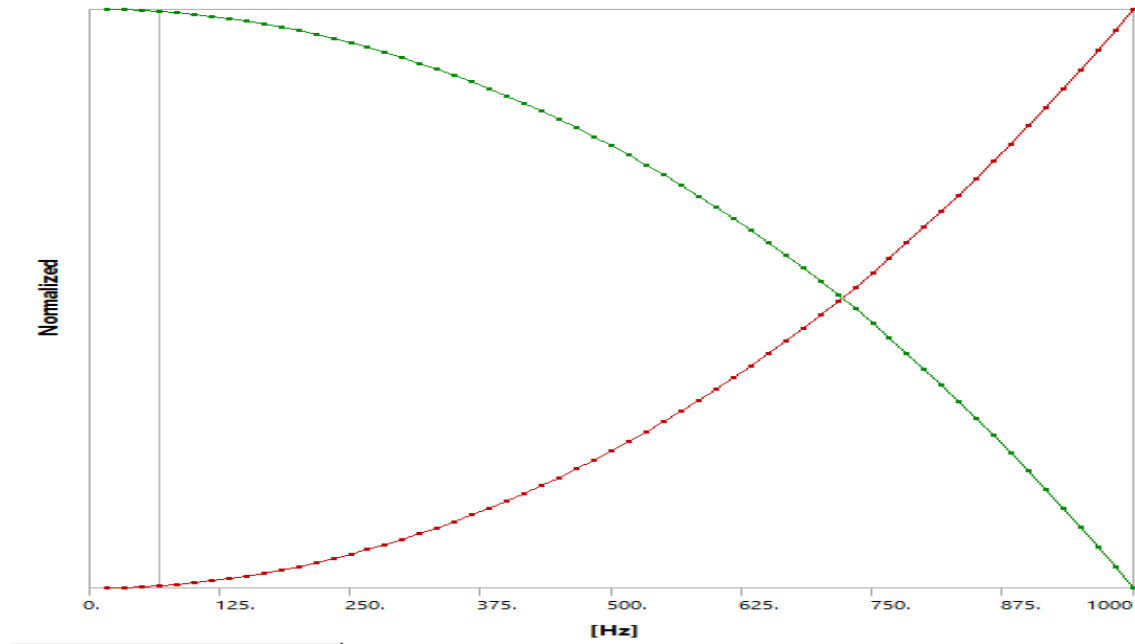


Fig.12 normalized natural and vibrational frequency to detect resonance condition

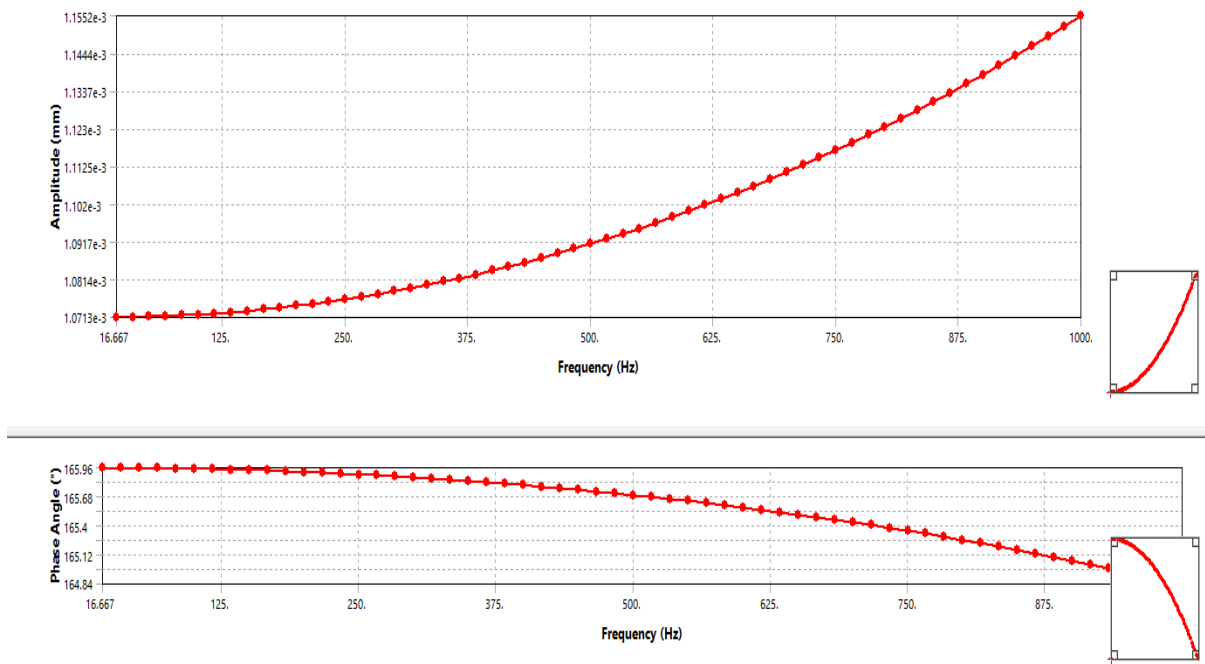


Fig.13 Variation of amplitude and phase angle with frequency for the applied loads.

7. Conclusion

- Thermal control analysis indicates that the components did not overheat in the hot case simulation because onboard components were mostly low-power devices.
- The structural analysis results indicate that the material used on the CubeSat should be able to withstand the loads throughout the launch period. Also, when the values of the physical deformation are looked at, they only vary slightly, therefore negligible with respect to the integrity of the structure during launch. The critical points of deformation seem to occur at the side top edges of the structure, but pose no threat as the material is strong enough to withstand the loads.
- Using topology optimization, we obtained a 24% mass reduction compared to the standard model, retaining 76% of the structural mass. This is a significant achievement in terms of environmental regulation and from an economic and sustainability point of view. Further measures could be taken to eliminate stress concentration and increase the fatigue life of the optimized structure.
- A harmonic study of normalized natural and vibrational frequency detect a resonance condition at 728 Hz. Appropriate measures should be taken to avoid resonance.

Finally, the results obtained are an indication that the structure is able to safely withstand the worst-case scenario.

8. Future Scope of work

Although numerical simulation can be used as a guide for designing the CubeSat, actual thermal testing of the system is still needed to ensure that the system can operate without failure. Looking ahead, the electronics will likely continue to shrink while adding more power and functionality. It is expected that future designs of CubeSats will include high-powered components to accommodate more sophisticated missions. We can carry out the further advanced studies by using the theory of inertia relief to study the effect of G-forces after the launch, when the spacecraft is unconstrained. We also find the Equivalent Radiated Power (ERP) results to estimate the radiated structure-borne sound power from vibrating structural surface and plot ERP as a function of frequency.

9 References

- [1] D. G. Gilmore, Spacecraft Thermal Control Handbook. California: The American Institute of Aeronautics and Astronautics.
- [2] Cihan ATAR and Metin AKTAS, Advances in Thermal Modeling and Analysis of Satellites. Journal of Science.
- [3] Jennifer Young, Scott Inlow and Brett Bender, Solving Thermal Control Challenges for CubeSats: Optimizing Passive Thermal Design.

- [4] Blake A. Moffitt, PREDICTIVE THERMAL ANALYSIS OF THE COMBAT SENTINEL SATELLITE, 16th 1 AIAA/USU Conference on Small Satellites,
- [5] J.Puig-Suari, C.Turner, R.J.Twiggs, CubeSat: The Development and Launch Support Infrastructure for Eighteen Different Satellite Customers on One Launch, AIAA/USU Conference on Small Satellites, 2001.
- [6] Armen Poghosyan*, Alessandro Golkar, CubeSat evolution: Analyzing CubeSat capabilities for conducting science missions. Progress in Aerospace Sciences.
- [7] Philipp Reiss, Philipp Hager, Malcolm Macdonald and Charlotte Lucking, New Methodologies for the Thermal Modelling of Cubesats. 26th Annual AIAA/USU Conference on Small Satellites. SSC12-VIII-5,
- [8] Sanjay Jayaram, SLUCUBE: Innovative high performance nanosatellite science and technology demonstration mission. Acta Astronautica 65 (2009) 1804 – 1812.
- [9] Patrick Hohn, Design and Validation of an articulated Solar panel for CubeSat. 29th Annual AIAA/USU Conference on Small Satellites, SSC15-P-41
- [10] Justin Likar, Stephen Stone, Robert Lombardi and Kelly Long, Novel Design Radiation Approach for CubeSat based Missions. 24th Annual AIAA/USU Conference on Small Satellites, SSC-10-III-1
- [11] Murat Bulut and Adem Kahriman, DESIGN AND ANALYSIS FOR THERMAL CONTROL SYSTEM OF NANOSATELLITE, Proceedings of the ASME 2010 International Mechanical Engineering Congress & Exposition IMECE2010, November 12-18, 2010, Vancouver, British Columbia, Canada
- [12] State of the Art of Small Spacecraft Technology, <https://www.nasa.gov/smallsat-institute/sst-soa-2020/thermal-control>.
- [13] Boris Yendler, Thermal control system, YSPM LLC, Saratoga, CA, United States.
- [14] Dinh Dai, "Thermal Modeling of Nanosat" (2012). Master's Theses. 4193
- [15] V. Chandrasekaran and Subramanian E.R., Transient Thermal Analysis of a Nano-Satellite in Low Earth Orbit. Proceedings of the Eighth International Conference on Engineering Computational Technology, B.H.V. Topping, (Editor), Civil-Comp Press, Stirlingshire, Scotland.
- [16] Devin T. Bunce, Kevin P. Bassett, Alexander R. M. Ghosh, Philip R. Barnett, Dawn M. Haken, Stephen Vrkljan, Rashi Jagannatha, Tiago Silva and Victoria L. Coverstone, Microvascular Composite Radiators for Small Spacecraft Thermal Management Systems. University of Illinois at Urbana Champaign , SSC16-X-1.

- [17] Karthigesu Thanarasi, Thermal Analysis of CUBESAT in Worse Case Hot and Cold Environment using FEA Method. *Applied Mechanics and Materials* Vol 225 (2012) pp 497-502
- [18] Andrew Rossi, Thermal Management Methods of Nanosatellites. *International Journal of Engineering and Technical Research (IJETR)* ISSN: 2321-0869, Volume-2, Issue-10, October 2014
- [19] Nur Athirah, M. Afendi, Ku Hafizan, N.A.M. Amin and M.S. Abdul Majid, Stress and Thermal Analysis of CubeSat Structure. *Applied Mechanics and Materials* Vol 554 (2014) pp 426-430
- [20] S. Corpino a,n , M. Caldera b , F. Nichele a , M. Masoero c , N. Viola a, Thermal design and analysis of a nanosatellite in low earth orbit. *Acta Astronautica*, 115(2015) 247-261.
- [21] Julio Balanzá, Jorge Prado-Molina, Jorge Prado-Morales, Juan Reyes, Structural Design and Analysis of a 3U Standardized CubeSat for a Future Mexican Mission. *SOMI Congreso De Instrumentacion*, Ano 4 No. 01, Octubre2017.
- [22] David Selčan*, Gregor Kirbiš, Iztok Kramberger, Nanosatellites in LEO and beyond: Advanced Radiation protection techniques for COTS-based spacecraft. *Acta Astronautica*, February 2017, Pages 131-144, vol 131
- [23] Derek W. Hengeveld, Mike R. Wilson, Jacob A. Moulton, Brent S. Taft and Andrew M. Kwas, Thermal design considerations for future high-power small satellites. 48th International Conference on Environmental Systems ICES-2018-77 8-12 July 2018, Albuquerque, New Mexico.
- [24] Luis A. Reyesa*, Roberto Cabriales-Gómez, Carlos E. Cháveza, B. Bermúdez-Reyesa, Omar López-Botello, P. Zambrano-Robledo, Thermal modeling of CIIASat nanosatellite: A tool for thermal barrier coating selection. *Applied Thermal Engineering*, 5 February 2020, 114651, vol 166.